CHIN. PHYS. LETT. Vol. 32, No. 9 (2015) 094201

High-Power Continuous-Wave Nd:GdVO$_4$ Solid-State Laser Dual-End-Pumped at 880 nm

MAO Ye-Fei(毛叶飞)[1], ZHANG Heng-Li(张恒利)[1**], SANG Si-Han(桑思晗)[1], ZHANG Xin(张新)[1],
YU Xi-Long(余西龙)[2], XING Ji-Chuan(邢冀川)[1], XIN Jian-Guo(辛建国)[1], JIANG Yi(江毅)[1]
[1] *School of Optoelectronics, Beijing Institute of Technology, Beijing 100081*
[2] *Institute of Mechanics, Chinese Academy of Sciences, Beijing 100190*

(Received 21 April 2015)

A high-power cw all-solid-state Nd:GdVO$_4$ laser operating at 880 nm is reported. The laser consists of a low doped level Nd:GdVO$_4$ crystal dual-end-pumped by two high-power diode lasers and a compact negative confocal unstable–stable hybrid resonator. At an incident pump power of 820 W, a maximum cw output of 240 W at 1064 nm is obtained. The optical-to-optical efficiency and slope efficiency are 40.7% and 53.2%, respectively. The M^2 factors in the unstable direction and in the stable direction are 4.38 and 5.44, respectively.

PACS: 42.55.−f, 42.55.Px, 42.55.Xi, 42.60.−v, 42.62.−b DOI: 10.1088/0256-307X/32/9/094201

Diode-laser (LD) end-pumped solid-state lasers (DPSSLs) have wide applications on the laser science and engineering community for their compactness, good beam quality, and high energy conversion efficiency. However, the power scaling of DPSSLs meets the problem of thermal effects with increasing incident pumped power. Some methods were introduced to reduce the thermal effects of the laser crystal, such as direct pump,[1] dual-end-pump[2] and composite crystal,[2−4] which were proved to be very efficient means. However, the most important is the laser media, which has excellent optical and thermal properties that are more suitable to be employed in high power DPSSLs.

Since a new Nd^{3+} host medium of GdVO$_4$, i.e. an isomorph of YVO$_4$, was first developed by Zagumennyi *et al.*[5] in 1992, it is becoming a promising laser crystal because of its advantageous appearance. Compared with Nd:YVO$_4$, Nd:GdVO$_4$ crystal has almost entirely similar lasing properties, while much higher absorption coefficient and larger emission cross section. Furthermore, most importantly, Nd:GdVO$_4$ crystal is characterized by its relatively broader gain bandwidth (1.3 nm) and unexpectedly high thermal conductivity along $\langle 110\rangle$ directions (about 11.7 W·m^{-1}K^{-1}), which was measured to be comparable with Nd:YAG. This feature makes it possible to avoid, to a great extent, the difficulties related to pump-induced thermal lensing in power scaling of diode-pumped solid-state lasers. In 2010, Li *et al.* reported a 46 W TEM$_{00}$ by a direct dual-end-pumped Nd:GdVO$_4$ laser with a grown-together composite crystal.[2] In 2014, a 149 W output power was achieved with $M^2 = 2.3$ in both directions.[6]

In this Letter, we report the high-power continuous-wave emission in Nd:GdVO$_4$ at 1064 nm under dual-end-pump by diode lasers at 880 nm directly into the $^4F_{3/2}$ emitting level.

Under direct dual-end-pump, a high slope efficiency of 53.2% and a maximum output power of 240 W were achieved while the incident pumped power was 820 W, leading to an optical-to-optical conversion efficiency of 40.7%. The M^2 factors in the horizontal direction and in the vertical direction are 4.38 and 5.44, respectively.

+A simple compact negative confocal unstable–stable hybrid resonator with a diode-double-end-pumped structure, as shown in Fig. 1, was used in our experiment. In a high-power solid-state laser system, laser gain media with low doped levels have better performance than those with high doped levels.[7] The low absorption coefficient of a low-doped-level laser crystal can uniformly distribute in the pumping beam, and mitigate the thermal problem, which is very important for a high power diode-pumped solid-state laser. Moreover, it can also tolerate very high incident pump power. Thus a 14 mm×10 mm×1 mm Nd:GdVO$_4$ crystal with a Nd-doped level as low as 0.5 at.% was used as the laser gain medium. The Nd:GdVO$_4$ crystal was a-cut with the c axis along the 14 mm direction. Both ends (14 mm×1 mm) were polished and coated with anti-reflection coating for the pump light and the laser light. The whole crystal was tightly wrapped in a water-cooled copper mount with two large faces 14 mm×10 mm. An indium foil was used to improve the thermal contact between the Nd:GdVO$_4$ crystal and the copper heat sink. The laser diode stack consisted of six bars with the central wavelength fixed at 880 nm by adjusting the cooling water temperature. The emission from each diode laser bar was individually collimated by a micro lens, which was coupled into a coupling system. The pump coupling system was similar to that used in Ref. [8] and led to a pump power loss of ∼10%. By the coupling system, we obtained a homogeneous pumping line of ∼0.4 mm×14 mm coupled into the Nd:GdVO$_4$ crystal. Temperatures of LD stacks and laser crystal were controlled by cooling circulating water. The fold hybrid resonator consisted of the input mirror (M1), 45° high-reflection mirror (M3) and the output mirror (M2). M1 was a concave mirror with a radius of 180 mm, which was coated for high reflection (HR) at

---

[**] Corresponding author. Email: zhl040325@bit.edu.cn

© 2015 Chinese Physical Society and IOP Publishing Ltd

1064 nm and high transmission (HT) at 880 nm. M2 was also a 140 mm concave mirror that was HR at 1064 nm. M3 was a flat mirror which was 45° HR coated at 1064 nm at surface b and HT coated at 880 nm at surface a. The folded resonator was an off-axis negative confocal unstable resonator in the horizontal direction and a stable direction in the vertical direction. In theory, the length of the resonator was $L = (R1+R2)/2 = 160$ mm. The equivalent transmission of the resonator was $T = 1 - |R2/R1| = 22.2\%$.

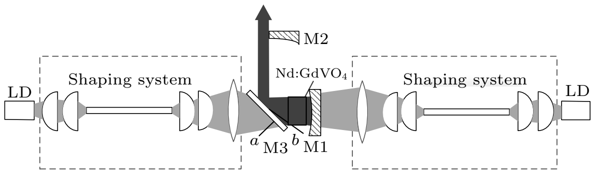

Fig. 1. Scheme of the experimental arrangement.

Part of the absorbed pumping energy would be transferred into heat dissipated in the laser crystal due to the quantum defect. The copper heat sink around the periphery of the crystal was water-cooled to keep at a constant temperature. The schematic view of Nd:GdVO$_4$ slab geometry is shown in Fig. 2. Consider that the thermal conductivity of the heat sink is much greater than of the crystal. The temperature at the cooling face of the crystal was supposed to be a constant. The heat conduction in the crystal can then be analyzed by the Poisson equation

$$K_x \frac{\partial^2 T(x,y,z)}{\partial x^2} + K_y \frac{\partial^2 T(x,y,z)}{\partial y^2} + K_z \frac{\partial^2 T(x,y,z)}{\partial z^2} + q(x,y,z) = 0, \tag{1}$$

where $q(x,y,z)$ is the thermal density arising from the pumping power, and K_x, K_y, K_z are the heat conductivities of the crystal in x, y, z orientations, respectively. The thermal density $q(x,y,z)$ was assumed to be of Gaussian function along the resonator axis in the crystal[9]

$$q(x,y,z) = \frac{2Q\alpha}{\pi\omega_{\rm p}^2}(1-e^{-\alpha l})e^{-2(x^2+y^2)/\omega_{\rm p}^2}e^{-\alpha z}, \tag{2}$$

where Q is the thermal load contributed from the portion of the incident power entering into the pumped face, α is the absorption coefficient for the pump light, $\omega_{\rm p}$ is the Gaussian beam waist, l is the crystal length. The specific parameters are listed in Table 1.

Table 1. Geometrical and physical properties of 0.5 at% Nd:GdVO$_4$ crystal.[10,11]

Width mm	Thickness mm	Length mm	Refractive index
c=10	b=1	a=14	n_0=1.972
Temperature coefficient (K)	Thermal expansion coefficients (K^{-1})	Thermal conductivity (W·m^{-1}K^{-1})	Absorption coefficient (cm^{-1})
dn/dt=4.7×10^{-6}	a_a=1.5×10^{-6}, a_c=7.3×10^{-6}	K_a=9.63, K_c=11.70	α=10 (808 nm), α=4 (880 nm)

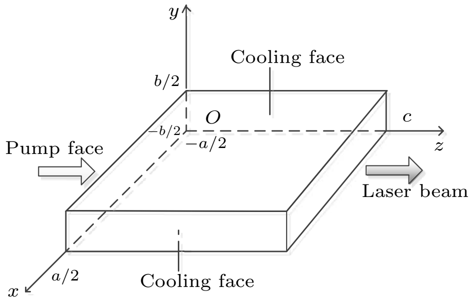

Fig. 2. Schematic view of the Nd:GdVO$_4$ slab geometry.

Equation (1) can be solved numerically by the Dirichlet method.[12] Suppose that the heat temperature is kept at $T_0 = 291$ K (18℃), both side facets (10 mm×1 mm) of the crystal were heat-insulated as they were directly exposed to air. The thermal distribution in the Nd:GdVO$_4$ crystal was numerically calculated under the condition of 820 W incident pumping power. The results are shown in Fig. 3.

The temperature difference of about 44℃ for the 880 nm LD single-end-pumped scheme, of about 76℃ for the 808 nm LD dual-end-pumped scheme and of about 22℃ for the 880 nm LD dual-end-pumped scheme are displayed in Fig. 3. Obviously, the direct pump and dual-end-pump are an effective method to reduce the thermal effects of the laser crystal and uniform in the heat distribution in the laser crystal.

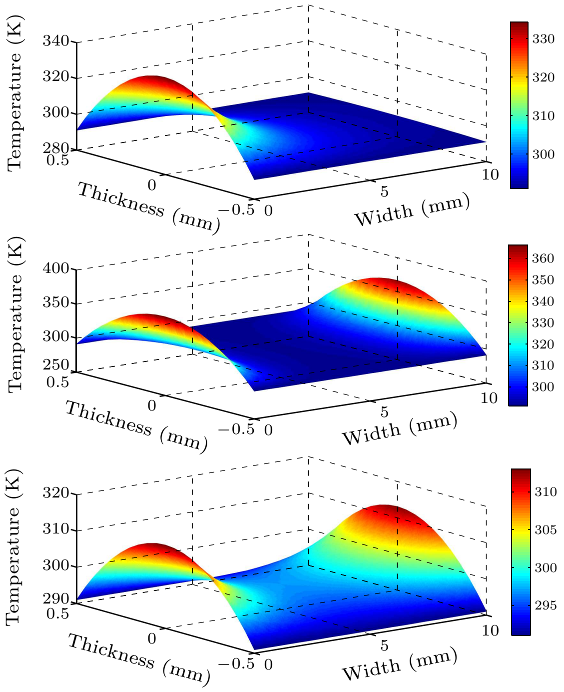

Fig. 3. The thermal distribution: (a) 880 nm single-end-pumped, (b) 808 nm dual-end-pumped, and (c) 880 nm dual-end-pumped.

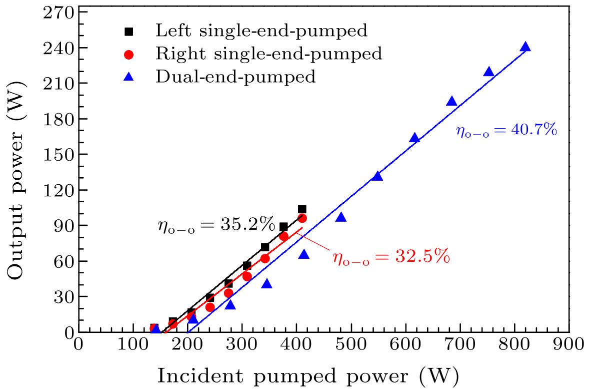

Fig. 4. The output power versus the incident pumping power.

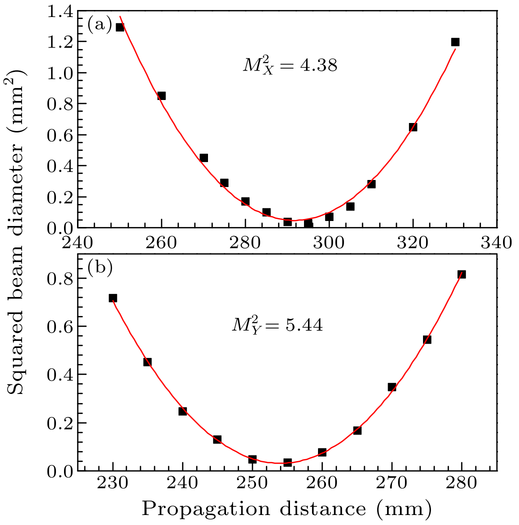

Fig. 5. The beam qualities of two directions: (a) horizontal (unstable) direction of hybrid resonator; (b) vertical (stable) direction of hybrid resonator.

The output power versus the pumping current is shown in Fig. 4. The maximum output powers of 104 W and 96 W at the incident pump power of 410 W for the left and right single-end-pumped were achieved, respectively. When taking the transmission efficiency (about 90%) of the coupling system and the absorption efficiency (about 80%) of the incident pumping power into account, the optical conversion efficiencies were 35.2% and 32.5%, respectively. The reason for the difference was the mode matching. A maximum output power of 240 W at the incident pump power of 820 W for the dual-end-pumped was obtained. When taking the transmission efficiency (about 90%) of the coupling system and the absorption efficiency (about 80%) of the incident pumping power into account, the optical-to-optical efficiency and slope efficiency were 40.7% and 53.2%, respectively. Due to the advantage of the dual-end-pump, the maximum output power is better than the total of the left and right single-end-pumped output power at the same current.

To measure the beam quality, a CCD camera was used to measure the laser spot widths at different positions behind an $f = 350$ mm spherical mirror. As M^2 was defined[13] by $d^2(z) = d_0^2(1 + (4M^2\lambda z/\pi d_0^2)^2)$, where d_0 is the beam diameter, z is the distance to the beam waist, $d(z)$ is the beam diameters at a distance z from the beam waist, d_0 is the beam diameter of beam waist and is the wavelength of laser, the squared beam diameters at different positions in both directions at output power of 240 W were obtained with the CCD, and were fitted as shown in Fig. 5. The beam quality M^2 factors in the unstable direction and the stable direction were 4.38 and 5.44, respectively.

In conclusion, dual-end-pumped and a negative confocal unstable–stable hybrid resonator were used. A 240 W 1064 nm laser output power is carried out with the pumped power of 820 W. The optical-to-optical efficiency and slope efficiency are 40.7% and 53.2%, respectively. The beam quality M^2 factors in unstable direction and stable direction are 4.38 and 5.44, respectively.

References

[1] Lupei V, Pavel N, Sato Y and Taira T 2003 *Opt. Lett.* **28** 2366
[2] Li X D, Yu X, Chen F, Yan R P, Luo M, Yu J H and Chen D Y 2010 *Opt. Express* **18** 7407
[3] Tsunekane M, Taguchi N and Inaba H 1996 *Electron. Lett.* **32** 40
[4] Lee H C, Brownlie P L, Meissner H E and Rea E C 1991 *Proc. SPIE* **1624** 2
[5] Zagumennyi A I, Ostroumov V G, Shcherbakov I A, Jensen T, Meyn J P and Huber G 1992 *Sov. J. Quantum Electron.* **22** 1071
[6] Deng B, Zhang H L, Xu L, Mao Y F, He J L and Xin J G 2014 *Chin. Phys. Lett.* **31** 114201
[7] Chen Y F 1999 *IEEE J. Quantum Electron.* **35** 234
[8] Cui L, Zhang H L, Xu L, Li J, Yan Y, Duan C, Sha P F and Xin J G 2010 *Chin. Phys. Lett.* **27** 114204
[9] Sugiyama A, Fukuyama H, Sasuga T, Arisawa T and Takuma H 1998 *Appl. Opt.* **37** 2407
[10] Zhang H J, Meng X L, Zhu L and Yang Z H 1999 *Mater. Res. Bull.* **34** 1589
[11] Gong C B, Chen C S, Wu B, Zhang Q L, Wu X Y and Yin S T 2005 *Chin. Opt. Lett.* **3** 94
[12] Mathews J and Fink K 2001 *Numer. Methods Using MATLAB* 3rd edn (Beijing: Publishing House of Electronics Industry)
[13] Hodgson N and Weber H 2005 *Laser Resonators Beam Propag.* 2nd edn (Berlin: Springer)